Talanta 84 (2011) 558–564

Contents lists available at ScienceDirect

Talanta

journal homepage: www.elsevier.com/locate/talanta

Inner filter effect of gold nanoparticles on the fluorescence of quantum dots and its application to biological aminothiols detection

Le Xu, Baoxin Li*, Yan Jin

Key Laboratory of Analytical Chemistry for Life Science of Shaanxi Province, School of Chemistry and Materials Science, Shaanxi Normal University, Xi'an 710062, People's Republic of China

ARTICLE INFO

Article history:
Received 2 October 2010
Received in revised form 21 January 2011
Accepted 25 January 2011
Available online 1 February 2011

Keywords:
Fluorescence
Inner filter effect
Gold nanoparticles
Quantum dots
Aminothiols

ABSTRACT

We have demonstrated the design of a new type fluorescence assay based on the inner filter effect (IFE) of gold nanoparticles (AuNPs) on the fluorescence of quantum dots (QDs). With a high extinction coefficient, AuNPs are expected to be capable of functioning as powerful absorbers. QDs with tunable emission wavelength are ideal fluorophores because the emission spectra of the rationally synthesized QDs can perfectly overlap with the absorption band of the absorber. Aminothiols are chosen as the model analytes, and the IFE-based fluorescent method for detection of aminothiols was suggested. Under the optimum conditions, the response is linearly proportional to the concentration of cysteine in the range of 0.05–0.9 $\mu g\,mL^{-1}$. The present IFE-based fluorescent strategy could be also used to detect glutathione and homocysteine. The linear concentration ranges were 0.05–1.0 $\mu g\,mL^{-1}$ for glutathione and 0.01–1.0 $\mu g\,mL^{-1}$ for homocysteine.

1. Introduction

The emergence and recent advance of nanoscience and nanotechnology open new opportunities for the application of nanomaterials in bioanalysis and biosensing [1,2]. Among nanomaterials, colloidal semiconductor nanocrystals (quantum dots, QDs) and gold nanoparticles (AuNPs) are especially attractive [3–5]. QDs display superior luminescence properties, such as size-dependent tunable photoluminescence, broad excitation spectra, narrow emission bandwidths and good photostability. So, QDs are the ideal candidates for signal generation and transduction in the fluorescent detection of analytes. With their great extinction coefficients, AuNPs are usually used in colorimetric-based detection systems [3,6–8]. Recently, AuNPs have been favorably adopted as an active unit in the fluorescent assays [9–15], and the most frequently adopted scheme is based on the ultra-efficient quenching capability of AuNPs to the fluorescence of nearby organic fluorophores through non-radiative energy/electron transfer processes [16]. It is well known that, compared with organic dyes, QDs have about 10–20 times brighter fluorescence and 100–200 times better photostablity [17]. So, some research groups have constructed fluorescence resonance energy transfer (FRET) between QDs and AuNPs, and have applied the FRET systems to sensitively detect biologically important analytes [18–21]. It is noted that the design of these FRET processes would involve the intermolecular connection of QDs with AuNPs at a particular distance or geometry to enable the interaction between them. Therefore, it is necessary and important for the AuNPs to be modified or engineered so as to directly contact with or be indirectly linked to special modified QDs. However, the modifying steps make the method very complicated, time-consuming and expensive, and consequently restricted their practical applications [22].

In this work, we present an alternative approach to design fluorescent assays based on the inner filter effect (IFE) of AuNPs on the fluorescence of QDs, which is conceptually different from the previously reported AuNPs-based FRET systems. In this approach, AuNPs and QDs do not need to be modified (or labeled). Notably, this approach does not require the link of AuNPs with QDs, which offers considerable flexibility and more simplicity. The IFE of fluorescence refers to the absorption of the excitation and/or emission of light by absorbers in the detection system [23]. Although the IFE is usually considered as an annoying source of error in spectrofluorometry and should be avoided, some studies have demonstrated its application in developing novel fluorescence assays [22,24–31]. Generally, in the IFE-based approach, two dyes are employed, one absorbent, the other fluorescent. These two dyes must meet the requirement: the absorption band of the absorbent dye possesses a complementary overlap with the excitation and/or emission bands of the fluorophore. Because of the limited choice of dyes, it is not easy to find the suitable absorber–fluorophore pair. Furthermore, the conventional absorber usually has a small extinction coefficient, which restricts the sensitivity of the IFE-based fluorescent assay.

* Corresponding author. Tel.: +86 29 85308184; fax: +86 29 85307774.
E-mail addresses: lbx29@hotmail.com, libaoxin@snnu.edu.cn (B. Li).

0039-9140/$ – see front matter © 2011 Elsevier B.V. All rights reserved.
doi:10.1016/j.talanta.2011.01.061

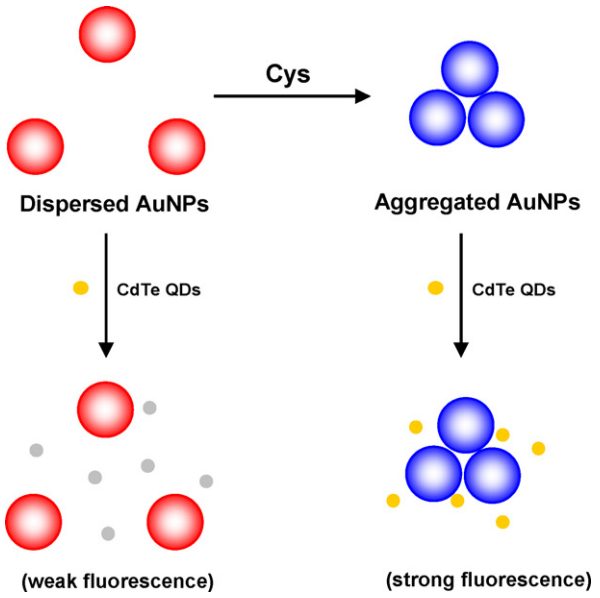

Scheme 1. Schematic representation of the IFE-based fluorescence assay for detection of Cys.

Therefore, the application of this IFE-based fluorescent assay is not very extensive. To the best of our knowledge, there are only about ten published papers on the IFE-based fluorescent assays.

AuNPs have tremendously lager extinction coefficient (e.g., the extinction coefficient of 13 and 30 nm-diameter particles is reported to be $2.7 \times 10^8\ M^{-1}\ cm^{-1}$ at 520 nm and $3.7 \times 10^9\ M^{-1}\ cm^{-1}$ at 520 nm, respectively [32]), which is much larger than that of the conventional chromophores. It is obvious that AuNPs can be used as ideal absorber in the IFE-based fluorescent assay. On the other hand, compared with conventional organic fluorescent dyes, QDs exhibit remarkable luminescence properties. In particular, the emission wavelengths of QDs can be tuned by size, composition, and shape [33], which result in high flexibility in the selection emission wavelength as well as maximum overlap with the absorption band of the absorbent dye. This attractive characteristic enables QDs to be a potential powerful and ideal fluorophore in the IFE-based fluorescent assay. Herein, we present one proof-of-concept example, in which AuNPs and QDs are used as absorber and fluorophore of the IFE-based fluorescent assay, respectively. We hypothesize that the changes in the absorbance of AuNPs can translate into the exponential changes in the fluorescence of QDs, and an enhanced sensitivity for the analytical method is reasonable with respect to the absorbance alone. This work is expected to open new opportunities for the development of the QDs fluorescence-based assay.

The low-molecular-mass aminothiols such as cysteine (Cys), homocysteine (Hcy) and glutathione (GSH) play a critical role in many biochemical pathways [34,35]. Their levels in biological fluids are important for clinical diagnostics of a variety of diseases. In this work, we develop a fluorescent method for detecting aminothiols through the IFE of AuNPs on the fluorescence of CdTe QDs. The principle of our method is shown in Scheme 1. The fluorescence of CdTe QDs is very weak in the presence of AuNPs due to the intensive absorption of AuNPs. In the presence of aminothiols (such as Cys), AuNPs will interact with aminothiols, thereby inducing the aggregation of AuNPs, which then leads to the decreased absorption of AuNPs' at ca. 527 nm [36]. In this case, the CdTe QDs exhibits the strong fluorescence emission. Therefore, the absorbance signal is easily converted into the fluorescence signal, which is used to detect aminothiols.

2. Experimental

2.1. Apparatus

All fluorescence measurements were performed using a Hitachi F-4600 fluorescence spectrophotometer (Tokyo, Japan) with a xenon discharge lamp at room temperature (ca. 20 °C). A 1.0 cm path length rectangular quartz cell was used for these measurements. UV–visible spectra were recorded on a Hitachi U-3900H spectrophotometer (Tokyo, Japan). Zeta potentials were recorded with a Nanoseris instrument (Malvern, England). Transmission electron microscopy (TEM) images of nanoparticles were acquired on a JEM-2100 transmission electron microscope (Tokyo, Japan). The pH measurements were carried out on model PB-10 digital ion analyzer (Sartorius Scientific instruments Co., Ltd., China, Beijing).

2.2. Materials

Homocysteine and sodium tellurite were purchased from Sigma (St. Louis, MO, USA). Cysteine, glutathione and chloroauric acid ($HAuCl_4$) were purchased from Shanghai Chemical Reagent Company (Shanghai, China). Sodium citrate and sodium chloride were purchased from Beijing Chemical Reagent Company (Beijing, China). Other amino acids were purchased from Shanghai Kangda Amino acid Factory (Shanghai, China). All other chemicals were of analytical grade and used without further purification. The water used was purified through a Millipore system.

2.3. Preparation of AuNPs

All glassware used in the following procedure was cleaned in a bath of freshly prepared 3:1 HNO_3–HCl, rinsed thoroughly in water and dried in air. AuNPs were prepared by the citrate reduction method according to the published protocol [37]. Briefly, a sodium citrate solution (1%, 500 μL) was rapidly added to a boiled $HAuCl_4$ solution under vigorous stirring. The mixed solution was boiled for 10 min, and further stirred for 15 min. The resulting solution was cooled to room temperature and filtered, which was stored in the refrigerator (4 °C) and ready for use. The different molar ratios of $HAuCl_4$/sodium citrate were used for the preparation of different nanometer-sized AuNPs. The size of AuNPs was measured by TEM.

2.4. Preparation of CdTe QDs

CdTe QDs were synthesized according to the reported method [38]. Four millilitres of 0.04 M cadmium chloride was diluted to 50 mL water in a one-necked flask, and trisodium citrate dihydrate (0.1 g), glutathione (0.05 g), Na_2TeO_3 (0.01 M, 1 mL) and $NaBH_4$ (0.05 g) were added with stirring. The mixture was reacted at 90 °C under open-air conditions for a certain period of time. For the purified CdTe QDs samples, the free $CdCl_2$ and GSH were removed via dialysis for 2 days in 0.01 M NaOH solution. A dialysis membrane with a molecular weight of cutoff 8000 was used for the purification of CdTe QDs. The final concentration of QDs was 3.7×10^{-4} M according to the TeO_3^{2-} concentration, and then kept at 4 °C in the dark for later use.

2.5. Fluorescence investigation on the interaction between CdTe QDs and AuNPs

2.0×10^{-4} M CdTe QDs in phosphoric buffered saline (PBS, pH 8.0, 0.01 M) was mixed with different concentrations of as-prepared AuNPs (ca. 40 nm) and equilibrated for 10 min. Then the emission spectra were recorded. The fluorescence data were analyzed by plotting the decreased fluorescence intensity at 530 nm

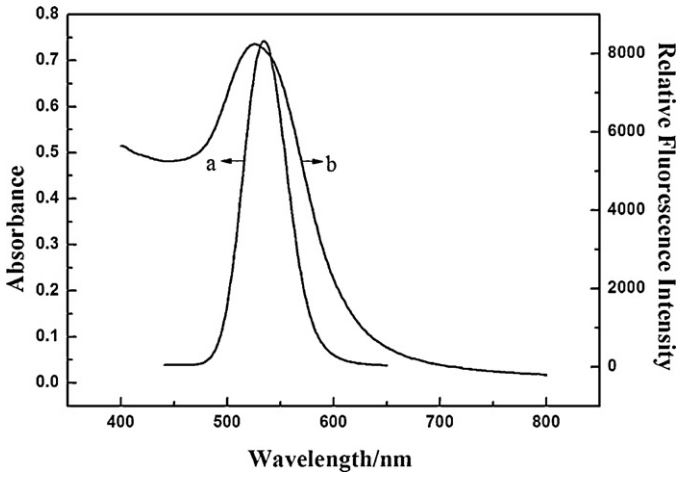

Fig. 1. Fluorescence emission spectra (a) of CdTe QDs and absorption spectrum (b) of AuNPs in PBS buffer (0.01 M, pH 8.0). CdTe QDs, 3.7×10^{-6} M, λ_{ex} = 350 nm; AuNPs, 1.6×10^{-10} M.

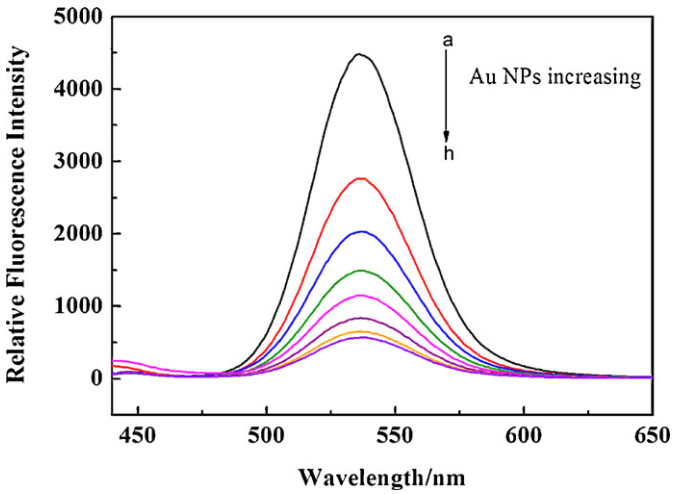

Fig. 2. Fluorescence emission spectra of QDs in the presence of increasing concentrations of AuNPs (ca. 40 nm): (a) 0 nM; (b) 0.47 nM; (c) 0.96 nM; (d) 1.9 nM; (e) 2.8 nM; (f) 3.5 nM; (g) 4.7 nM; (h) 10 nM. CdTe QDs, 9.1×10^{-7} M, λ_{ex} = 350 nm.

versus the concentration of AuNPs. To investigate the effect of emission wavelength on the fluorescence decrease by AuNPs, a series of fluorescence experiments of CdTe QDs under the emission wavelength from 490 to 602 nm were performed.

2.6. Fluorescent detection of aminothiol

A typical fluorescent analysis was realized by following steps. First, 100 μL AuNPs (ca. 40 nm) solution was adjusted to acidic with 30 μL HAc (0.01 M), and then mixed with 100 μL aminothiol (such as Cys) with different concentrations. This mixture solution was allowed to react for 15 min at room temperature. Second, 50 μL CdTe QDs (1.87×10^{-5} M) was added to the above prepared solution, and then the obtained solution was diluted with PBS (pH 8.0, 0.01 M) to 1.0 mL. The resulting solution was incubated for 10 min at room temperature before spectral measurements. The instrument excitation and emission slits were set at 10 nm, and the fluorescent spectrum and intensity were obtained with excitation wavelength of 350 nm at room temperature. The concentration of aminothiol was quantified by the increased fluorescence intensity (ΔF, $\Delta F = F - F_0$, where F and F_0 are the fluorescence intensity of the system at 530 nm in the presence and absence of aminothiol, respectively).

3. Results and discussion

3.1. Optical characteristics of AuNPs and CdTe QDs

Fig. 1 shows the absorption spectrum of AuNPs and the fluorescence emission spectrum of CdTe QDs. Aqueous AuNPs (ca. 40 nm) display an intense plasmon absorption (λ_{max} = 527 nm) and appear pink. In the present study, AuNPs are adopted as the absorber. The fluorescence emission wavelength of CdTe QDs could be easily tuned by changing the refluxing time. When the refluxing time was 45 min, we obtained the CdTe QDs with a maximum emission at 530 nm, which was just near the absorption maximum of AuNPs (Fig. 1). It can also be seen that the width of the fluorescence spectrum is narrow (the width at half-maximum is about 40 nm), showing that the QDs are monodisperse and uniform. The average particles size is about 2.97 nm, based on the empirical fitting function from the previous report [39]. It is obvious that the emission spectrum of CdTe QDs overlaps nicely with the absorption spectrum of AuNPs. Thus, the effective emission intensity of CdTe QDs would be more decreased if the two materials coexist.

3.2. Effect of AuNPs on the fluorescence of CdTe QDs

As shown in Fig. 2, the emission intensity of CdTe QDs decreases gradually with increasing the concentration of AuNPs. In this work, AuNPs were prepared by the citrate reduction method. AuNPs in aqueous solution are stabilized against aggregation due to the negative capping agent's (citrate ion) electrostatic repulsion against van der Waals attraction between AuNPs [40]. So, AuNPs possess negative charge, which was supported by the zeta potential of AuNPs (the dispersed 40-nm AuNPs exhibited the zeta potential of −40.5 mV). At the same time, we measured the zeta potential of the CdTe QDs, and the zeta potential of the GHS-capped CdTe QDs was −29.4 mV in pH 8.0 PBS, due to the ionization of the –COOH group in GHS (pK_a 3.6 [41]). Thus, there is not electrostatic interaction between the negatively charged AuNPs and the negatively charged CdTe QDs. Very recently, the study [20] in Guo's group demonstrated that the positively charged QDs could form the FRET donor–acceptor assemblies with negatively charged AuNPs by electrostatic interactions because the electrostatic interaction could shortened the distance between the QDs donor and the AuNPs acceptor. So, an efficient FRET process did not occur between the negatively charged AuNPs and the negatively charged CdTe QDs in this present system. Furthermore, no complex formation was expected between QDs and AuNPs in this system, which was supported by the fact that absorption spectrum of AuNPs did not change in the presence of QDs. Therefore, the observed fluorescence decrease should be mainly to the IFE of AuNPs on the fluorescence of CdTe QDs. With increasing the concentration of AuNPs, the absorbance of the absorber increased, which would shield the emission light from CdTe QDs. As a result, the emission intensity of CdTe QDs decreased.

We also compared the effect of AuNPs on the fluorescence emission of CdTe QDs with different sizes. It is well known that the emission wavelength depends on the size of CdTe QDs. As shown in Fig. 3, which plotted the fluorescence change of CdTe QDs with difference maximum emission wavelength versus the concentration of AuNPs, the results suggest a decreasing extent following the order: $QDs_{E530\,nm} > QDs_{E490\,nm} > QDs_{E580\,nm} > QDs_{E602\,nm}$. This order accords well with the absorbance characteristic of AuNPs (the absorption maximum of AuNPs is at 527 nm). The AuNPs absorbed the emission light at 530 nm more intensity than at the other wavelengths. This fact also provided the further support that the emission of CdTe QDs was decreased by AuNPs mainly via the IFE. Notably, in the presence of AuNPs as low as 0.067 nM, the fluo-

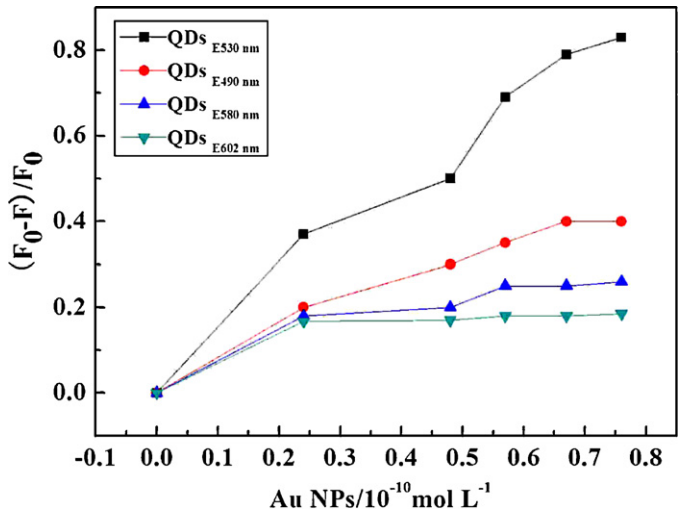

Fig. 3. Fluorescence quenching efficiency versus AuNPs concentration and CdTe QDs with different emission wavelengths. CdTe QDs, 9.1×10^{-7} M, λ_{ex} = 350 nm.

rescence intensity of CdTe QDs decreased by over 65%. This could be attributed to the high extinction coefficient of AuNPs, which is one advantage of using AuNPs as the absorber compared with conventional chromophores. Therefore, the fluorescence of CdTe QDs at 530 nm can be tuned by the absorbance of AuNPs via IFE. Compared to the complicated and costly QDs–AuNPs FRET process [18–21], this kind of IFE strategy is very simple.

3.3. Absorbance of AuNPs in the presence of Cys

Fig. 4 presents the absorption spectrum of AuNPs in the presence of Cys with different concentrations. It can obviously been seen that Cys can induce the decrease of absorbance of AuNPs at 527 nm, and the decreased extent increases with increasing concentration of Cys. Furthermore, when Cys concentration is higher than 0.09 μg mL^{-1}, a new absorbance peak appears in the long-wavelength band (~730 nm). It is well known that the surface plasmon absorption of AuNPs is very sensitive to their interparticles distance [36]. Highly dispersed AuNPs (effectively considered as single particles) in solution exhibit only a single peak, while linked Au pairs (formation of Au dimers or trimers) show

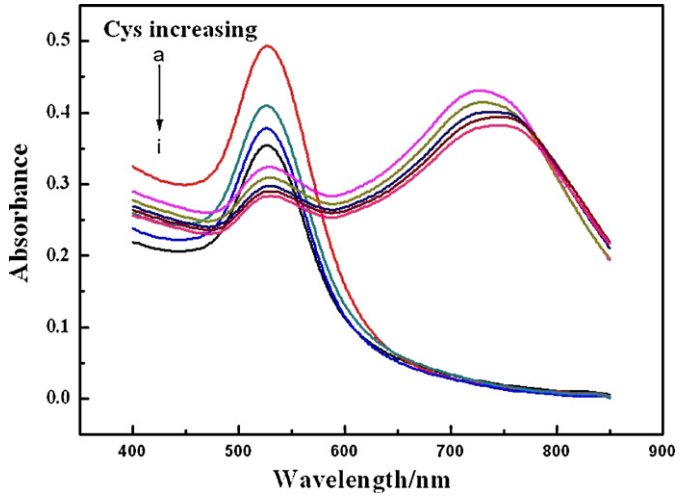

Fig. 4. Absorption spectra of AuNPs in the presence of Cys with different concentrations: (a) 0 μg mL^{-1}; (b) 0.05 μg mL^{-1}; (c) 0.07 μg mL^{-1}; (d) 0.09 μg mL^{-1}; (e) 0.10 μg mL^{-1}; (f) 0.30 μg mL^{-1}; (h) 0.50 μg mL^{-1}; (i) 0.70 μg mL^{-1}; (j) 0.90 μg mL^{-1}. AuNPs, 0.48×10^{-7} M; HAc, 1.3 mM.

two absorbance maxima. The first peak, located near 520 nm, is attributed to quadrupole plasmon excitation in coupled spheres, while the second peak at a longer wavelength is attributed to the dipole plasmon resonance of the AuNPs [42]. As the interparticles spacing decreases, the first peak becomes weaker [36]. The thiol group exhibits intriguing reactivity reaction with AuNPs, and Cys can easily bind onto the gold surface through the sulfur atom [43]. And then, the intermolecular hydrogen-bonding and/or zwitterionic electrostatic interactions between the amino acids attached onto AuNPs can induce the aggregation of AuNPs [44].

In order to know the microstructure of the AuNPs without and with Cys, the TEM images (Fig. 5) were obtained. Note that in the absence of Cys, the AuNPs are mono-dispersed, whereas the AuNPs aggregate together in the presence of Cys. The results were consistent with the change of the UV–visible absorption spectra (Fig. 4), and the color of the AuNPs solution changed from red to purple in the presence of high concentration Cys. Furthermore, the experimental results showed that Hcy and GSH also could induce the decrease of the absorbance of AuNPs at 527 nm. Therefore, upon emission at 530 nm, the fluorescence of CdTe QDs, can be tuned by the aminothiol–AuNPs system via IFE, which provides a new strategy for fluorescent detection of aminothiols (Cys, Hcy and GSH).

3.4. Fluorescence detection of aminothiols through the IFE of AuNPs on the fluorescence of CdTe QDs

We designed a fluorescent aminothiols assay based on the analyte-induced decrease of the absorbance of the absorber (AuNPs), which then recovered the IFE-decreased fluorescence of the fluorophore (CdTe QDs). As shown in Fig. 6A, the fluorescence intensity of AuNPs–QDs increases gradually with increasing the concentration of Cys, which corresponds with a gradual decrease on the plasmon absorbance of AuNPs (Fig. 4). Meanwhile, no discernible change in the shape of the emission spectra is observed in the presence of Cys and AuNPs. So, it can be indicated that the increased emission came from the CdTe QDs rather than any other newly formed emission centers. On the other hand, the effect of Cys on fluorescence of QDs (in the absence of AuNPs) was also studied, and the experimental results showed that Cys could not enhance the fluorescence intensity of the CdTe QDs in the absence of AuNPs. Thus, the increased fluorescence should originate from the interaction between Cys and Au NPs which then affected the emission of the CdTe QDs.

The performance of the developed sensing for aminothiols was strongly influenced by the assay conditions such as media pH, AuNPs concentration, CdTe QDs concentration and binding time. We investigated the effect of these factors. Media pH not only affects the interaction between aminothiols and AuNPs, but also influences the interparticle assembly of the aminothiols-attached AuNPs. Our study showed that Cys could not induce the obvious change of surface plasmon absorption of AuNPs in alkali media, and Cys could decrease the absorbance of AuNPs at 527 nm, which could be due to the effect of pH on hydrogen-bonding and/or electrostatic interactions between the amino acids attached onto AuNPs [45]. Amine group (–NH_2) in all amine acids can bind AuNPs only at relative low pH (pH < 2.0), whereas the thiol group (–SH) can bind AuNPs at high pH [36]. So, in order to eliminate the influence of other amino acids on the detection of aminothiols, we chose 1.3 mM HAc (pH 3.8) as the interaction media of aminothiols with AuNPs. On the other hand, the media pH also affects the fluorescence of CdTe QDs. The experimental results showed that the AuNPs–CdTe QDs fluorescence system presented the most sensitivity for detection of aminothiols at 0.01 M PBS (pH 8.0). Thus, in the whole process for detecting aminothiols, aminothiols firstly interact with AuNPs in 1.3 mM HAc, then the reaction was changed to

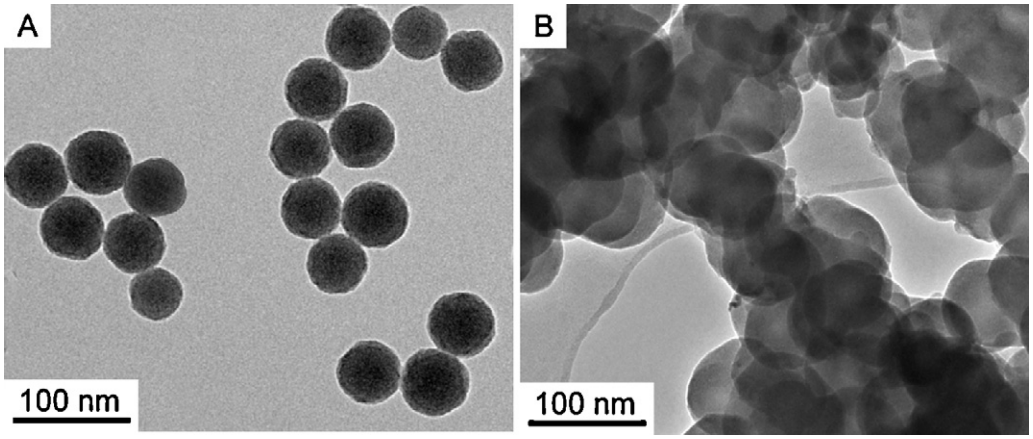

Fig. 5. TEM image of Au NP before (A) and after (B) adding Cys. AuNPs, 4.8×10^{-8} M; Cys, 1.0×10^{-6} g mL^{-1}; HAc, 1.3 mM.

0.01 M PBS (pH 8.0) for measuring fluorescence of the AuNPs–CdTe QDs system.

We used three different nanometer-sized gold colloids (2.6 nm, 13 nm and 40 nm) to study the effect of Au particle size on analytical performance of Cys. The experimental results showed that larger AuNPs were more sensitive to the target molecular (Cys). This is possibly due to that the fluorescence quenching ability of AuNPs is strongly size-dependent and larger AuNPs quench the fluorescence of nearby fluorophore more efficiently [46]. So, we chose 40 nm AuNPs as the probes. We also investigated the effect of AuNPs concentration and CdTe QDs concentration on the fluorescence response. The experimental results showed that a higher concentration of AuNPs could decrease the background fluorescence, but the response for Cys with low concentration was weak. On the other hand, a lower concentration of AuNPs could enhance the response for Cys with low concentration, but the background fluorescence was higher, and the dynamic range was found to be narrower. The optimal concentrations of AuNPs and QDs were 4.6×10^{-11} M and 9.1×10^{-7} M, respectively. Finally, we optimized the incubation time of Cys–AuNPs binding and AuNPs–CdTe QDs interaction. For low concentration of Cys (500 nM), the absorption of AuNPs at 527 nm reached a minimum in 15 min; after addition of CdTe QDs to the above AuNPs solution, the AuNPs–QDs mixture was incubated for 10 min, and the fluorescence intensity of the system at 530 nm reached a maximum.

Under the above optimum conditions, the analytical parameters of the present method for Cys detection were then investigated. As shown in Fig. 6B, a good linear relationship between the increased fluorescence intensity ($\Delta F = F - F_0$) and the Cys concentration is obtained in the range of 0.05–0.9 μg mL^{-1}. The detection limit was 8 ng mL^{-1} (3σ). The relative standard deviation for 11 repeated measurements of 0.1 μg mL^{-1} Cys was 2.5%, which illustrated that the response of AuNPs–QDs to Cys was highly reproducible. It is noteworthy that the present method provided a much lower detection limit than the previously reported absorbance-based method for Cys detection using AuNPs (~40 nm) as colorimetric probes [36]. In addition, the presence of common species, including Na^+, K^+, Mg^{2+}, Ca^{2+}, Cl^-, NO_3^-, CO_3^{2-}, PO_4^{3-}, glucose, lactose and lactic acid (5.0 μM), could not interfere with detecting 0.1 μg mL^{-1} Cys. Fe^{3+} and Cu^{2+} (5.0 μM) yielded little or low interference to Cys detection using this method. The possible reason is that Fe^{3+} or Cu^{2+} can oxidize Cys.

The selectivity of this method was evaluated by testing the response of the assay to other α-amino acids. The experimental results are shown in Fig. 7. It is clear that amino acids with thiol group (Cys, Hcy and GHS) give an increased fluorescence signal, while there is nearly no observable fluorescence change upon the addition of other amino acids without thiol group at the identical concentration. The main reason is that only amino acids possessing two functional groups (–NH_2 and –SH) can act as cross-linking agents for pairs of AuNPs under the proposed experimental conditions [36]. Therefore, the above method was also employed to determine the concentrations of Hcy and GHS. The linear concentration ranges were are 0.05–1.0 μg mL^{-1} for GSH and 0.01–1.0 μg mL^{-1} for Hcy, and the equations of the calibration curves were $\Delta F = 157.4 + 27.4\ c_{GHS}$ (where c_{GHS} is GSH concentration, μg mL^{-1}; $r = 0.9961$) and $\Delta F = 141 + 62.9\ c_{Hcy}$ (where c_{Hcy} is Hcy concentration, μg mL^{-1}; $r = 0.9984$). The limits of detection (3σ) were 5.0×10^{-9} g mL^{-1} and 3.0×10^{-9} g mL^{-1} for GSH and Hcy, respectively.

In order to test our proposed method in real samples, we studied the potential applicability of this assay for the direct determination of thiols in human plasma. The fresh human blood samples from some volunteers were collected from Shaanxi Normal University Hospital and used as testing samples. The human blood samples with added EDTA were centrifuged at 4000 rpm for 10 min. The supernatant solution containing proteins and amino acids was collected and used as the source of plasma. For determination of total aminothiols, the disulfide bonds were reduced in order to release the protein-bound thiols by addition of triphenylphosphine as catalyst [47,10]. Briefly, 500 μL of the collected plama were vigorously mixed with 40 μL of 0.2 M HCl and with 20 μL of 0.4 M triphenylphosphine (in water–acetonitrile 20:80 (v/v) and 2.0 M HCl). After incubating for 15 min the hydrolysed plasma was mixed with

Table 1
Determination of total aminothiols in human plasma samples using QDs-AuNPs fluorescence system.

Sample	Determined aminothiols (10^{-5} g mL^{-1})	Added Cys (10^{-5} g mL^{-1})	Measured (10^{-5} g mL^{-1})	Recovery (%)	RSD ($n = 6$, %)
1	6.89	4.00	10.99	101	3.1
		6.00	12.79	99	3.9
2	10.43	4.00	13.80	96	3.0
		6.00	16.51	100	4.2
3	13.91	4.00	18.11	101	2.9
		6.00	18.98	95	3.9

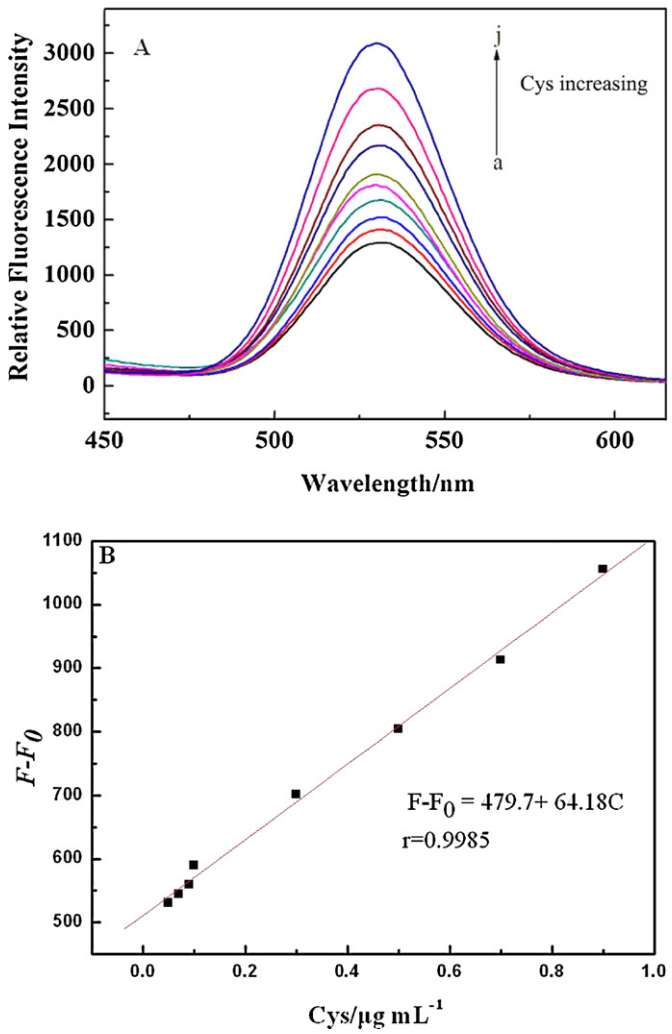

Fig. 6. Fluorescence emission spectra of AuNPs–QDs system in the presence of increasing concentrations of Cys (A) and linear plots of increased fluorescence intensity ($F-F_0$) at 530 nm versus the concentration of Cys (B). CdTe QDs, 9.1×10^{-7} M; AuNPs, 4.6×10^{-11} M; Cys (a–j): 0, 0.05, 0.07, 0.09, 0.10, 0.30, 0.50, 0.70, 0.90, and 2.5 μg mL^{-1}.

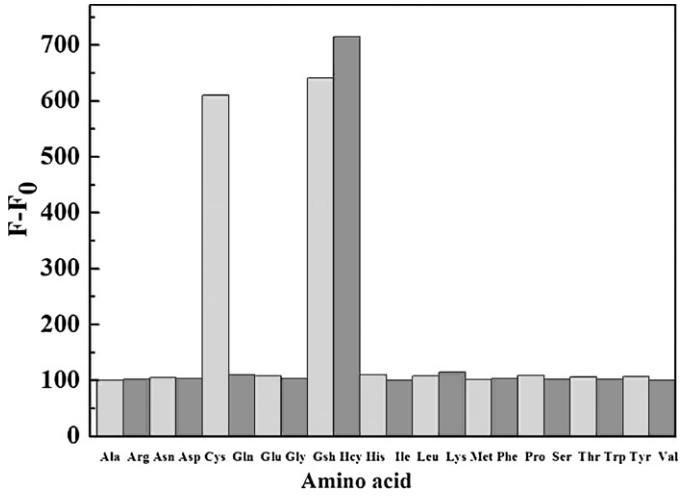

Fig. 7. The increased fluorescence intensity ($F-F_0$) of AuNPs–QDs at 530 nm in the presence of 5.0×10^{-7} g mL^{-1} amino acids. CdTe QDs, 9.1×10^{-7} M; AuNPs, 4.6×10^{-11} M.

500 μL of acetonitrile to precipitate proteins, followed by centrifugation at 4000 rpm for 20 min. The supernatant which contained aminothiols in plasma was used for further analysis The concentrations of aminothiols in three different plasma samples were determined by the standard addition method using Cys as the standard, since Cys is known as the main component of aminothiols in human plasma. The results were listed in Table 1. The recovery of added known amount Cys to the plasma samples was in the range of 95%–101%, which suggested the accuracy and reliability of the present method for aminothiol determination in practical applications.

4. Conclusions

In this work, we have demonstrated the feasibility of developing a new fluorescent assay using the inner filter effect of AuNPs on CdTe QDs for first time. By employing aminothiols as the model analyte, we show that AuNPs can function as a powerful absorber in the IFE-based fluorescent assay to turn the emission of fluorophore with high sensitivity. On the same time, QDs are proved to be an ideal fluorophore in the IFE-based fluorescent assay because the emission wavelengths of QDs can be easily tuned by size and composition, thereby resulting in high flexibility in the selection emission wavelength as well as maximum overlap with the absorption band of the absorbent dye. The present IFE-based strategy allows the design of fluorescent assays in a more simple, time-saving, and economical approach, since no modification (or labeling) step of AuNPs and QDs. Moreover, it is anticipated that the present concept can be generalized to design fluorescent assays for sensing a wide range of AuNPs-involved events such as interparticles aggregation/deaggregation, shape/size evolvement, and surface adsorption/desorption.

Acknowledgements

This project is supported the Key Project of Chinese Ministry of Education (No. 109150) and the Fundamental Research Funds for the Central Universities (No. GK2009011004).

References

[1] C. Burda, X. Chen, R. Narayanan, M.A. El-Sayed, Chem. Rev. 105 (2005) 1025–1102.
[2] T. Asefa, C.T. Duncan, K.K. Sharma, Analyst 134 (2009) 1980–1990.
[3] W.A. Zhao, M.A. Brook, Y.F. Li, Chembiochem 9 (2008) 2363–2371.
[4] R. Gill, M. Zayats, I. Willner, Angew. Chem. Int. Ed. 47 (2008) 7602–7625.
[5] W. Zhong, Anal. Bioanal. Chem. 394 (2009) 47–59.
[6] H. Li, L.J. Rothberg, Proc. Natl. Acad. Sci. 101 (2004) 14036–14039.
[7] X. Xu, M.S. Han, C.A. Mirkin, Angew. Chem. Int. Ed. 46 (2007) 3468–3470.
[8] X. Xue, F. Wang, X. Liu, J. Am. Chem. Soc. 130 (2008) 3244–3245.
[9] J. Zhang, L. Wang, H. Zhang, F. Boey, S. Song, C. Fan, Small 6 (2010) 201–204.
[10] L. Shang, J. Yin, J. Li, L. Jin, S. Dong, Biosens. Bioelectron. 25 (2009) 269–274.
[11] M. Wang, W. Hou, C.C. Mi, W.X. Wang, Z.R. Xu, H.H. Teng, C.B. Mao, S.K. Xu, Anal. Chem. 81 (2009) 8783–8789.
[12] Y.M. Chen, T.L. Cheng, W.L. Tseng, Analyst 134 (2009) 2106–2112.
[13] C.C. Huang, S.H. Chiu, Y.F. Huang, H.T. Chang, Anal. Chem. 79 (2007) 4798–4804.
[14] H. Wang, Y. Wang, J. Jin, R. Yang, Anal. Chem. 80 (2008) 9021–9028.
[15] S.Y. Lim, J.H. Kim, J.S. Lee, C.B. Park, Langmuir 25 (2009) 13302–13305.
[16] E. Dulkeith, A.C. Morteani, T. Niedereichholz, T.A. Klar, J. Feldmann, S.A. Levi, F.C.J.M. van Veggel, D.N. Reinhoudt, M. Möller, D.I. Gittins, Phys. Rev. Lett. 89 (2002), 203002-1–203002-4.
[17] A.M. Smith, S. Nie, Analyst 129 (2004) 672–677.
[18] L. Shi, V.D. Paoli, N. Rosenzweig, Z. Rosenzweig, J. Am. Chem. Soc. 128 (2006) 10378–10379.
[19] E. Oh, M.Y. Hong, D. Lee, S.H. Nam, H.C. Yoon, H.S. Kim, J. Am. Chem. Soc. 127 (2005) 3270–3271.
[20] X. Wang, X. Guo, Analyst 134 (2009) 1348–1354.
[21] E. Oh, D. Lee, Y.P. Kim, S.Y. Cha, D.B. Oh, H.A. Kang, J. Kim, H.S. Kim, Angew. Chem. Int. Ed. 45 (2006) 7959–7963.
[22] L. Shang, S. Dong, Anal. Chem. 81 (2009) 1465–1470.
[23] P. Yuan, D. Walt, Anal. Chem. 59 (1987) 2391–2394.
[24] L. Shang, C. Qin, L. Jin, L. Wang, S. Dong, Analyst 134 (2009) 1477–1482.

[25] N. Shao, Y. Zhang, S.M. Cheung, R.H. Yang, W.H. Chan, T. Mo, K.A. Li, F. Liu, Anal. Chem. 77 (2005) 7294–7303.
[26] H. He, H. Li, G. Mohr, B. Kovács, T. Werner, O.S. Wolfbeis, Anal. Chem. 65 (1993) 123–127.
[27] X.F. Yang, P. Liu, L. Wang, M. Zhao, J. Fluoresc. 18 (2008) 453–459.
[28] G. Gabo, D.R. Walt, Anal. Chem. 63 (1991) 792–796.
[29] K. Tohda, H.W. Lu, Y. Umezawa, M. Gratzl, Anal. Chem. 73 (2001) 2070–2077.
[30] Y. Xiang, Z. Li, X. Chen, A. Tong, Talanta 74 (2008) 1148–1153.
[31] X. Yang, K. Wang, C. Guo, Anal. Chim. Acta 407 (2000) 45–52.
[32] U. Kreibig, L. Genzel, Surf. Sci. 156 (1985) 678–700.
[33] J.M. Klostranec, W.C.W. Chan, Adv. Mater. 18 (2006) 1953–1964.
[34] S. Zhang, C.N. Ong, H.M. Shen, Cancer Lett. 208 (2004) 143–153.
[35] G.C. Han, Y. Peng, Y.Q. Hao, Y.N. Liu, F.M. Zhou, Anal. Chim. Acta 659 (2010) 238–242.
[36] Z. Zhong, S. Patskovskyy, P. Bouvrette, J.H.T. Luong, A. Gedanken, J. Phys. Chem. B 108 (2004) 4046–4052.
[37] L. Li, B. Li, Analyst 134 (2009) 1361–1365.
[38] J. Yuan, W. Guo, J. Yin, E. Wang, Talanta 77 (2009) 1858–1863.
[39] W. Wu, L. Qu, W. Guo, X. Peng, Chem. Mater. 15 (2003) 2854–2860.
[40] A. Ono, H. Togashi, Angew. Chem. Int. Ed. 43 (2004) 4300–4302.
[41] R.M.C. Dawson, D.C. Elliott, W.H. Elliott, K.M. Jones, Data for Biochemical Research, Clarendon Press, Oxford, 1959.
[42] T. Jensen, L. Lelly, A. Lazarides, G.C. Schatz J., Clusters Sci. 10 (1999) 295–317.
[43] K. Uvdal, P. Bodö, B. Liedberg, J. Colloid Interface Sci. 149 (1992) 162–173.
[44] F.X. Zhang, L. Han, L.B. Israel, J.G. Daras, M.M. Maye, N.K. Ly, C.J. Zhong, Analyst 127 (2002) 462–465.
[45] I.I.S. Lim, D. Mott, W. Ip, P.N. Njoki, Y. Pan, S. Zhou, C.J. Zhang, Langmuir 24 (2008) 8857–8863.
[46] P.P.H. Cheng, D. Silvester, G. Wang, G. Kalyuzhny, A. Douglas, R.W. Murray, Phys. Chem. B 110 (2006) 4637–4644.
[47] A.R. Ivanov, I.V. Nazimova, L. Baratova, J. Chromatogr. A 895 (2000) 157–166.